IOP Conf. Series: Materials Science and Engineering **375** (2018) 012025 doi:10.1088/1757-899X/375/1/012025

Comparison of rolling texture of austenite and ferrite phases of duplex steel with single-phase austenitic and ferritic steel

J Capek[1], M Cernik[2], N Ganev[1], K Trojan[1], J Nemecek[1], K Kolarik[1]

[1] Department of Solid State Engineering, Faculty of Nuclear Sciences and Physical Engineering, Czech Technical University in Prague, Trojanova 13, Prague, Czech Republic
[2] U. S. Steel Košice, s.r.o., Košice, Slovak Republic

E-mail: Jiri.Capek@fjfi.cvut.cz

Abstract. In this contribution, the behavior of three types of steel after rolling was investigated. Ferritic and austenitic steels or phases have different mechanical and thermal properties. Due to their mutual influence during plastic deformation, it is possible to suppose the differences between preferred orientations of austenite and ferrite phases in duplex steel and single-phase austenitic and ferritic steels. For this reason, the preferred orientations of austenite and ferrite phases of rolled duplex steel were compared with rolled single-phase austenitic and ferritic steel. The 0–50% reductions of rolled steel plates were selected. Mainly, the strength and type of preferred orientation were compared in the relation to reduction and material. For this purpose, the rolled surfaces were measured by X-ray diffraction. The significant differences between intensities and types of texture components were investigated. For austenite-ferrite interaction during plastic deformation and phase transformation, samples were analysed by electron back-scattered diffraction. The Kurdjumov-Sachs orientation relationship was investigated.

1. Introduction

Duplex stainless steels or duplex steels are dual-phases steels with ferrite and austenite phases with roughly 50/50 proportion. Due to the combination of properties of both phases and two phase microstructure, duplex steels exhibit high corrosion and wear resistance in many environments, where the standard austenitic and ferritic steels are usually used [1]. For this reason, it is possible to manufacture lighter functional components. However, disadvantages are combined too. Due to austenite phase, duplex steels are susceptible to mechanical hardening and, because of ferrite phase, to hydrogen embrittlement.

The importance of study of preferred orientation (texture) originates in the anisotropy of most material properties. Consequently, the analysis and subsequent interpretation of the texture is crucial, especially in material engineering. Moreover, texture analysis during the thermo-mechanical processing of materials provides information on the basic mechanism. The properties, which are influenced, are the Young's modulus of elasticity, Poisson number, hardness, strength, ductility, abrasion resistance, magnetic permeability, electrical conductivity etc. Therefore, materials with a strong texture are used to produce components with specific properties [2]. Major deformation mechanisms responsible for the formation of ferrite and austenite rolling

textures in duplex steels should be similar as in the single-phase steels. However, austenite and ferrite phases are generally different in plastic and elastic properties. Therefore, their behavior during deformation can be different in comparison with single-phase steels [3].

2. Theory

Texture is interpreted in the form of orientation distribution function (ODF), pole figures, and inverse pole figure (IPF) maps. ODF is usually presented using Euler space, which is defined by three rotations of crystallites $\mathbf{g} = (\varphi_1,\ \Phi,\ \varphi_2)$, so called Euler angles in Bunge notation [2]. ODF or *f(***g***)* function determines the bulk density of crystals with the **g** orientation. The unit of *f(***g***)* is multiple of a random distribution, i.e. the function is normalized to one, which corresponds to the random orientation of crystals. According to crystal and sample symmetries, the Euler angles of materials with cubic crystal and orthorhombic sample symmetries are in the range $(\varphi_1,\ \Phi,\ \varphi_2) \in \langle 0°;\ 90° \rangle$. For materials with a face centered cubic (fcc) and a body centered cubic (bcc) lattice, the ODF is usually interpreted using different texture components and textures with fibre components, shortly fibres, [4], see Fig. 1. These fibres are usually interpreted according to rolling (RD), transversal (TD) and normal (ND) directions. The type and strength of texture are significantly dependent on the material structure (especially on the grain size and initial texture), chemical and phase composition, and mainly the thermo-mechanical properties of presented phases [2, 3, 5].

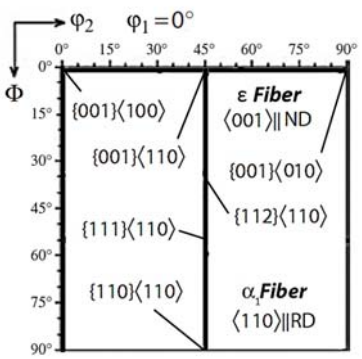

(a) $\varphi_1 = 0°$ section of bcc material

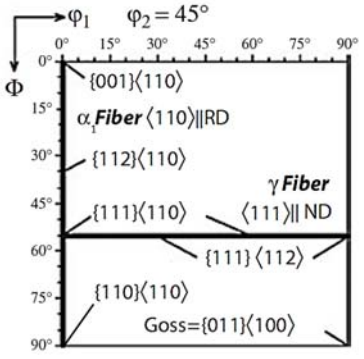

(b) $\varphi_2 = 45°$ section of bcc material

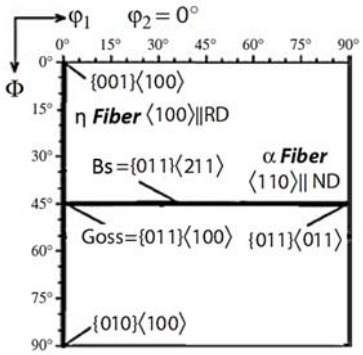

(c) $\varphi_2 = 0°$ section of fcc material

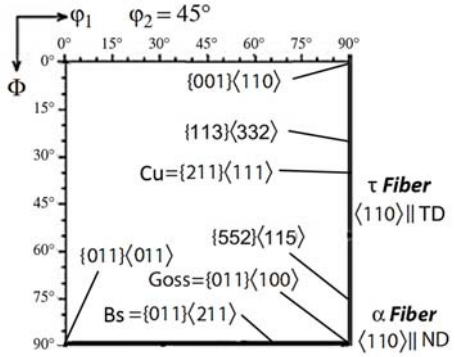

(d) $\varphi_2 = 45°$ section of fcc material

Figure 1: Representation of typical fibres and texture components of deformed cubic materials [2].

Typical orientations in deformed bcc materials are formed into three characteristic fibres. During cold rolling, primarily the α_1, ε and γ-fibres are created. The α_1-fibre is characterized by $\langle 110 \rangle \| \mathrm{RD}$ and includes e.g. the rotated cubic component $\{001\}\langle 110\rangle$. The γ-fibre includes crystallographic directions with $\{111\}$ planes which are parallel to ND. Rotated cubic component (or orientation) $\{001\}\langle 110\rangle$ and cubic component $\{001\}\langle 100\rangle$ are part of ε-fibre which is characterized by $\langle 100 \rangle \| \mathrm{ND}$.

The most important texture components for fcc materials of Brass type (materials with small stacking fault energy — SFE) are Goss (G) $\{011\}\langle 100\rangle$ and Brass (Bs) $\{\overline{1}10\}\langle 112\rangle$, see Fig. 1. In the paper [5], this Brass type is called Silver type (Ag). Less common texture component is Copper (Cu) $\{\overline{2}11\}\langle 111\rangle$, mostly for relatively high SFE. These texture components are part of three main texture fibres: α — $\langle 110 \rangle \| \mathrm{ND}$, τ — $\langle 110 \rangle \| \mathrm{TD}$ and η — $\langle 100 \rangle \| \mathrm{RD}$. The potentional difference between duplex and austenite steel may be caused by the difference in SFE, which depends on chemical composition. According to [6], the SFE of austenite steel is arround 18 mJ/m^2 and for γ phase of duplex steel, the SFE is 10 mJ/m^2.

The orientation relationship (OR) of all phases is necessary to known for interpretation of austenite-ferrite interaction. During the manufacturing of duplex steels, the samples are usually quenched. Therefore, the orientations of precipitated/transformed grains are not random. According to [7], solidification of duplex steels is controlled by chemical composition. So initially, the solid phase is completely ferritic (α). Subsequent cooling results in austenite phase (γ) generation in diffusion reaction $\alpha \rightarrow \alpha + \gamma$. According to temperature gradient during quenching and diffusion, four basic types of dual-phase structure can exist [7]. The most common structures are duplex and dispersion. The duplex structure is created by austenite grains precipitated on the grain boundaries of α phase. In the case of dispersion structure, not all dissolved elements, which stabilize the austenitic structure, diffuse on grain boundaries. From these elements, γ phase precipitate intergranular [7]. For this reason, the microstructure of typical duplex steel consists of α matrix with coarse intragranular (islands creating) and fine intergranular γ grains.

The orientation relationships (ORs) are usually represented in Rodrigues-Frank (R-F) space which is a map of all corresponded orientations and variants [8]. From R-F space is possible to reach information about differences between ORs, see Tab. 1. During most phase transformations, certain favoured orientation relationship exists between the parent and the daughter phases. The OR can be described according several models: Bain, Kurdjumov-Sachs (K-S), Nishiyama-Wasserman (N-W) etc., see Tab. 1. The Greninger-Troiano is called an irrational OR because of high Miller index numbers. The rest of ORs are called rational ORs due to low Miller indices. From a single-austenite crystal, 12 and 24 crystallographic variants can be formed with a N-W and K-S/Pitsch orientations relationship, respectively, due to the symmetry of cubic systems. By comparing all 12 variants, only five possible misorientation angles (MAs) (13.76°, 19.47°, 50.05°, 53.69° and 60°) between variants are maintained in the case of the N-W relationship [9]. For K-S orientations relationship, the MAs are about 4° smaller, i.e. 10.53° and 55.53° [8].

Each material may show its specific combination of nucleation OR and OR continuum [10]. In low-carbon steels the K-S OR nucleation is observed and the orientation gradually changes to a Pitsch variant [10]. Therefore, duplex steel proved to be useful for understanding ORs in steel, in which γ precipitations nucleate in a α matrix [11] and the K-S OR was predominantly found.

3. Experiment

The plate shape samples of size 19×120 mm^2 and different thicknesses were made of AISI 420 (ferritic), AISI 304 (austenitic) and AISI 318LN (duplex) type of stainless steel using grinding and milling. Before deformation, the austenitic and ferritic with duplex samples were annealed in air laboratory furnace for 4 hours at 840 °C and 7 hours at 650 °C, respectively, in order to

Table 1: Common orientation relationship models: Bain, Kurdjumov-Sachs, Nishiyama-Wassermann, Pitsch and Greninger-Troiano, where α and γ are ferrite and austenite phases, respectively [7].

OR	crystalographic planes	crystalographic directions	MA of α -γ
Bain	$\{001\}_\gamma \| \{001\}_\alpha$	$\langle 100\rangle_\gamma \| \langle 110\rangle_\alpha$	45°
Kurdjumov-Sachs	$\{111\}_\gamma \| \{011\}_\alpha$	$\langle 011\rangle_\gamma \| \langle 111\rangle_\alpha$	42.8°
Nishiyama-Wassermann	$\{111\}_\gamma \| \{011\}_\alpha$	$\langle 112\rangle_\gamma \| \langle 011\rangle_\alpha$	45.9°
Pitsch	$\{100\}_\gamma \| \{110\}_\alpha$	$\langle 110\rangle_\gamma \| \langle 111\rangle_\alpha$	45.9°
Greninger-Troiano	$\{111\}_\gamma \| \{110\}_\alpha$	$\langle 123\rangle_\gamma \| \langle 133\rangle_\alpha$	44.2°

reduce residual stresses. In the end, the samples were cold rolled with 0, 10, 20, 30, 40, and 50% reductions of thickness, thus the final thickness of all samples was 1.5 mm. Therefore, samples made of ferritic, austenitic and duplex steel were marked as F0–F50, A0–A50 and D0–D50, respectively.

X'Pert PRO MPD diffractometer with Co$K\alpha$ radiation was used to the analyses of RD-TD plane samples by X-ray diffraction (XRD). Texture analysis was performed based on ODF calculation from experimental pole figures which were obtained on three diffraction lines $\{110\}$ ($\{220\}$ for α phase in duplex steel), $\{200\}$, $\{211\}$ of ferrite phase and $\{111\}$ ($\{311\}$ for γ phase in duplex steel), $\{200\}$, $\{220\}$ of austenite phases. Irradiated volume of samples was based on size of primary slits (1×1 mm^2), geometry of experiment and penetration depth of the used radiation into given material, see [12].

Contrarily, the TD-ND plane of samples was investigated by electron backscatter diffraction (EBSD). The *TESCAN VEGA3* electron microscope with *NordlysMax3* EBSD camera was used for measurement of IPF maps. IPF maps were measured at magnification 250× and 1µm step due to a coarse-grain structure in duplex steels.

XRD and EBSD analysis was not done for mutual comparison, but served as complementary data. XRD data was primarily used for texture analysis and EBSD data for austenite-ferrite interaction. The MATLAB™ toolbox MTEX software was used for processing of all experimental data [13].

4. Results and discussions

4.1. X-ray diffraction

Dependence of relative intensities of texture fibres *f(***g***)* on the rolling reduction is shown in Figs. 2. In view of the fact that the typical texture components of rolled materials are part of texture fibres, only 2-D ODF sections of samples with 50% deformation are presented, see Figs. 3. For samples without deformation, it is possible to assume that the initial texture is composed of grinding texture components. The rolling texture was generated during rolling of the samples.

In the ferritic samples F0–F50, see Fig. 2a, the typical texture components and fibres were generated. It is evident that strength of the texture components and fibres are increasing with higher deformation. During cold rolling, the strong α_1 and γ-fibres were generated. The dominant texture component are $\{001\}\langle 110\rangle$ (rotated cubic), $\{\overline{1}12\}\langle 110\rangle$ and $\{\overline{1}11\}\langle 110\rangle$. The ε-fibre contains only representative rotated cubic component.

For the austenitic samples A0–A50, see Fig. 2c, the transition between grinding and rolling texture is evident. The rotated cubic component $\{001\}\langle 110\rangle$ is part of grinding texture. During deformation (rolling), grains rotate to the cubic orientation $\{001\}\langle 100\rangle$. From 30% deformation

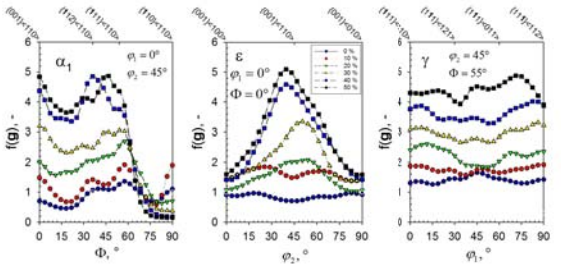

(a) Ferritic steel

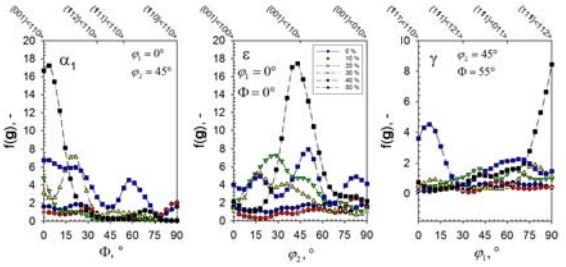

(b) Duplex steel — α phase

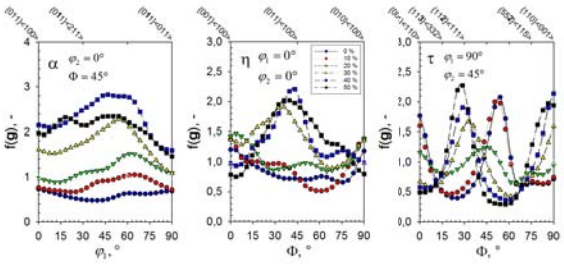

(c) Austenitic steel

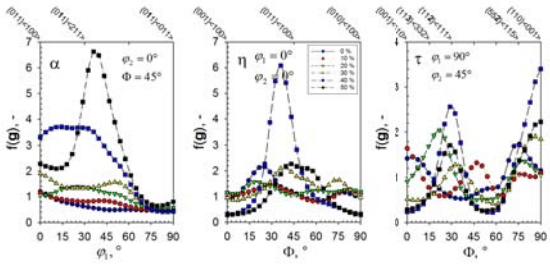

(d) Duplex steel — γ phase

Figure 2: ODFs along individual fibres (α_1, ε and γ) and (α, η and τ) of α and γ phases, respectively.

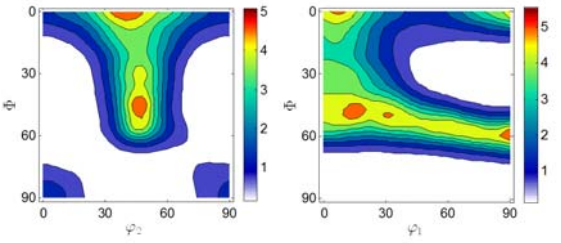

(a) Sample F50

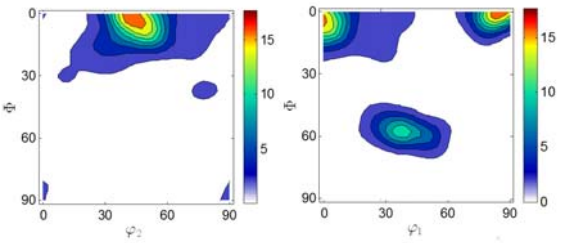

(b) Sample D50 — α phase

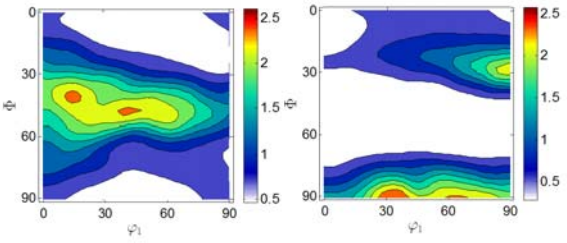

(c) Sample A50

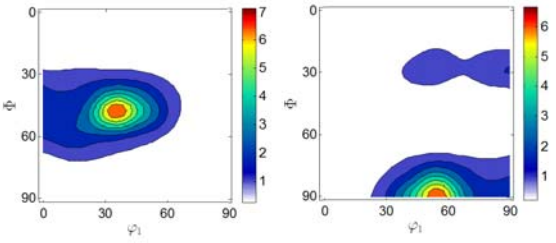

(d) Sample D50 — γ phase

Figure 3: Orientation distribution functions in the $\varphi_1 = 0°$ (left) and $\varphi_2 = 45°$ (right) sections for α phases, and $\varphi_2 = 0°$ (left) and $\varphi_2 = 45°$ (right) sections for γ phases.

the G component $\{110\}\langle 001\rangle$ is generated. Rotating these grains around $\langle 100\rangle \| \mathrm{RD}$ axis, the η-fibre is formed. The cubic component is a part of η-fibre too. If grains with G orientation rotate around $\langle 110\rangle \| \mathrm{ND}$ axis, the α-fibre and Bs texture component are generated. The τ-fibre is only composed of G and Cu texture components. Cu texture component is more common for materials with high SFE.

The differences in type and strength of texture of duplex steel are evident in comparison with single-phase steels from Figs. 2. In the case of ferrite phase (Fig. 2b), the mutual influence of α and γ phases and mainly different mechanical properties of both phases results in limitation of rotation of α grains during deformation. During rolling, the harder phase (α) keeps energy until deformation exceeds a certain limit. This released energy results in sudden α grains rotation to another discrete orientation. From this reason, the texture components are very strong and are not typical for this deformation for bcc materials or phases. However, typical texture component is generated in the sample with higher deformation, i.e. rotated cubic component $\{001\}\langle 110\rangle$, see Fig. 3b.

Texture components of γ phase of duplex steel (Fig. 2d) are stronger in comparison with single-phase steel which are caused by mutual interaction during plastic deformation. With increasing of deformation, only Bs, G and Cu texture components are generated. For the sample with 50% deformation, majority of grains have Bs orientation.

4.2. Electron backscatter diffraction

Using EBSD, the austenite-ferrite interaction was investigated. In Figs. 4 IPF maps of D0 and D50 samples are presented. The MAs of both phases are depicted in Figs. 5.

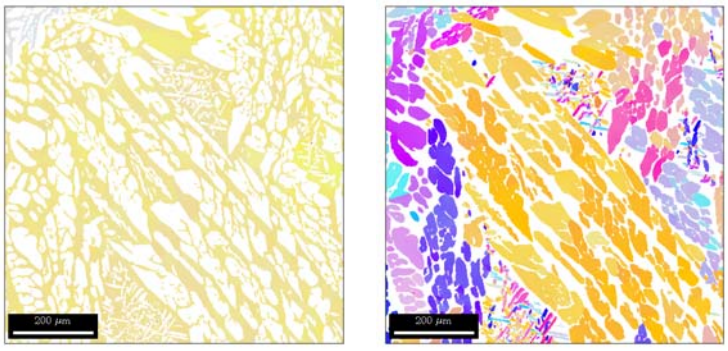

(a) Sample D0 — α phase (b) Sample D0 — γ phase

(c) Sample D50 — α phase (d) Sample D50 — γ phase

Figure 4: Inverse pole figure maps of α and γ phases of D0 and D50 samples.

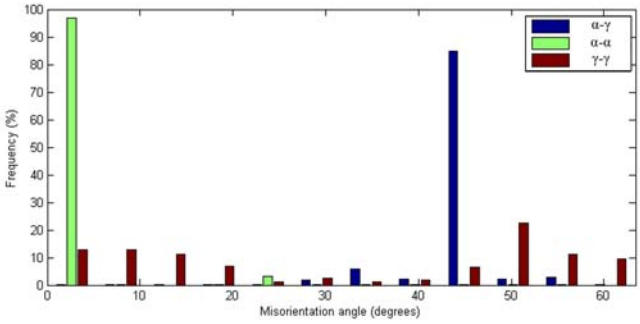

(a) Sample D0

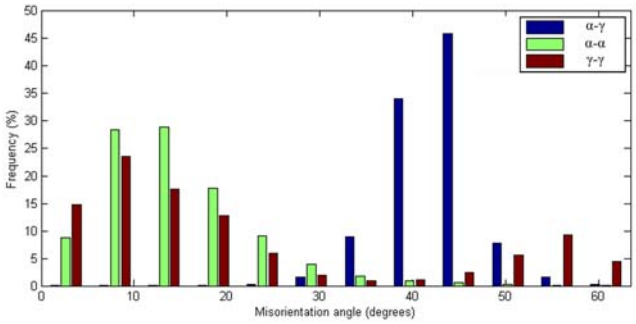

(b) Sample D50

Figure 5: Misorientation angles between γ -γ , α -γ and α -α phases of D0 and D50 samples.

From IPF maps in Figs. 4 and MA in Figs. 5, the solidification history of duplex steels is evident. According to the theory, see Section 2, initially, the solid is completely ferritic. This microstructure is composed of ferritic coarse-grain with small MA which is under 10°. During further cooling, the austenite grains are precipitated on the grain boundaries and in the grains and create duplex and disperse structure, respectively. Generally, the phase transformation is a solid-solid transformation with minimum diffusion, as supported by the high cooling rates. The orientation of γ grains is not random, but MAs between α and γ grains is around 43°, where the best fit is with K-S OR, see Tab. 1. According to K-S or N-W OR, the MAs between γ and γ grains are around 10° and 55°. Rest of MAs, i.e. mainly 20–40°, represents random orientations.

During deformation, the grains are re-oriented. The MAs between α and γ grains is not strictly 42.8°, but it creates Gaussian distribution. For high deformation, the MAs between α and α is similar to Gaussian distribution too with maximum at 10°. The MAs between γ and γ grains has the equal trend as the D0 sample. The MA function has maxima around 10° and 55°. These trends are typical for cubic materials and correspond with K-S (10.53° and 55.53°) or N-W (13.76° and 60°) OR.

5. Conclusions

Results obtained using XRD showed:

- The intensity and development of texture components are different for single and dual-phase types of steels.
- With increasing degree of deformation of single-phase samples, a considerable increase in the texture intensity was observed.

- For ferritic sample, there are four main texture components $\{001\}\langle 110\rangle$ (rotated cubic), $\{\overline{1}12\}\langle 110\rangle$, $\{\overline{1}11\}\langle 110\rangle$ and $\{11\overline{1}\}\langle 112\rangle$ which are parts of α_1, ε and γ-fibres.
- For α phase of duplex steel, only rotated cube component $\{001\}\langle 110\rangle$ is dominant after 50% deformation. The texture for α phase of duplex steel is stronger compared with ferritic samples.
- Texture of austenitic steel is primarily composed of expected Brass $\{110\}\langle\overline{1}12\rangle$, Goss $\{110\}\langle 001\rangle$ components and less common Copper $\{11\overline{2}\}\langle 111\rangle$ component which are parts of α, τ and η-fibres.
- In the case of γ phase of duplex steel, Goss, Brass and Copper texture components are also presented. But for high deformation, only Brass component develops texture, which is typical for steels with low SFE. These texture fibre components are not conspicuous.

Using EBSD analyses, further results were acquired:

- Microstructure of duplex steel is composed of α grains which have MA approx. 10°. During solidification, two types of γ grains precipitate. Firstly, on the grain boundaries (coarse-grains) and in the grains (disperse fine-grains).
- The MA of α -γ is 42.8° according to K-S OR.
- Because of plastic deformation during rolling, the MAs between α and γ grains after rolling are not strictly 42.8°, but it creates a Gaussian distribution.
- Behavior of MA of α -α and γ -γ grains is according to K-S or N-W OR with maxima at around 10° and 55°.

References

[1] Dakhlaoui R, Braham C and Baczmański A 2007 Mechanical properties of phases in austeno-ferritic duplex stainless steel-Surface stresses studied by X-ray diffraction *Mater. Sci. Eng.: A* **444** 6–17
[2] Bunge H J 1982 *Texture Analysis in Materials Science* (London: Butterworth)
[3] Ryś J, Ratuszek W and Witkowska M 2006 Comparison of the Rolling Texture Formation in Duplex Steels with Various Initial Textures *Arch. Metall. Mater.* **51** 495–502
[4] Suwas S and Ray R K 2014 *Crystallographic Texture of Materials* (Springer-Verlag)
[5] Hu H 1974 Texture of metals *Texture* **1** 233–58
[6] Reick W, Pohl M and Padilha A F 1996 Determination of stacking fault energy of austenite in aduplex stainless steel *steel res. int.* **67** 253–6
[7] Knyazeva M and Pohl M 2013 Duplex Steels: Part I: Genesis, Formation, Structure *Metallogr. Microstruct. Anal.* **2** 113–21
[8] He Y, Godet S, Jonas J J 2004 Representation of misorientations in Rodrigues-Frank space: application to the Bain, Kurdjumov-Sachs, Nishiyama-Wassermann and Pitsch orientation relationships in the Gibeon meteorite *Acta Mater.* **55** 1179–90
[9] Beladi H, Adachi Y, Timokhina I and Hodgson P D 2009 Crystallographic analysis of nanobainitic steels *Scripta Mater.* **60** 455–8
[10] de Jeer L T, Ocelík V and De Hosson J T 2017 Orientation Relationships in $Al_{0.7}$CoCrFeNi High-Entropy Alloy *Microsc. Microanal.* **23** 905–15
[11] Jiao H, Aindow M and Pond R C 2003 Precipitate orientation relationships and interfacial structures in duplex stainless steel Zeron-100 *Philos. Mag.* **83** 1867–87
[12] Čapek J and Pala Z 2014 Programs for Visualizing Results of Diffraction Experiments *Mater. Struct.* **21** 93–4
[13] Bachmann F, Hielscher R and Schaeben H 2010 Texture Analysis with MTEX — Free and Open Source Software Toolbox *Solid State Phenomen.* **60** 63–8

Acknowledgments

This work was supported by the Grant Agency of the Czech Technical University in Prague, grant No. SGS16/245/OHK4/3T/14, Czech Science Foundation, grant No. 14-36566G, and the "Nadání Josefa, Marie a Zdeňky Hlávkových" Foundation.